DIAGNOSTYKA, 2022. Vol. 23. No. 2

A METHODOLOGY FOR NON-INVASIVE DIAGNOSIS OF DIESEL ENGINES THROUGH CHARACTERISTICS OF STARTER SYSTEM PERFORMANCE

Juan D. RAMÍREZ *, **Carlos A. ROMERO** , **Juan C. MEJÍA** , **Héctor F. QUINTERO**

Universidad Tecnológica de Pereira, Colombia
* Corresponding author, e-mail: juandaviramireza@utp.edu.co

In this work, a methodology to diagnose ten diesel bus engines is carried out by means of some characteristics of the starting system performance. The signals of battery voltage, electric current supplied to the starter motor and crankshaft revolutions during cold and warm engine starting processes are analysed. Characteristics and patterns of the signals that are attributable to engine compression and combustion failures are pointed out, which are related to the kilometres travelled by each vehicle after the last engine repair and the shutdown time of the engine in warm condition. It is obtained that the rise of the current required by the starter motor during the second and third compression process, and the mean crankshaft angular acceleration after the second compression process are characteristics that are related to the engine condition.

Keywords: internal combustion engines, engine diagnosis, starting system, starting process.

1. INTRODUCTION

Internal combustion engines (ICE) are machines that convert some of the chemical energy of a fuel into mechanical energy.Despite strict environmental regulations, due to its portability, power and reliability, engines will continue to be used in heavy-duty applications, such as trucks, ships and emergency power generators, and in activities in isolated locations, such as agriculture and mining [1].

Diagnosis of ICE is necessary due to increasing demand and requirements for environmental, safety, reliability, and durability. A malfunctioning engine consumes more fuel, emits more pollutants, loses performance, and becomes unreliable. Through diagnostics and condition monitoring it is possible to increase reliability, improve efficiency, reduce costs and extend engine life [2]–[5].

Condition monitoring consists of monitoring and examining the performance of the ICE and the different systems, which allows detecting failures and scheduling the necessary intervention to correct potential problems even at an early stage [2], [6].

As diagnostic techniques, compression pressure measurement and oil analysis provide information about cylinder wear. However, their application requires engine intervention or partial disassembly, i.e. these techniques are invasive [4], [5]. By means of torque or engine power, faults can also be diagnosed [7]. Torque measurement is feasible on test benches equipped with dynamometers, i.e. the engine must be removed from the vehicle or the machine in which it operates, or from free acceleration tests, but it is necessary to know the

inertia moment of the mechanisms [5]. The analysis of acoustic and vibration signals are non-invasive techniques that carry information from different engine failures [2], [4], [5], [8]–[10]. However, signal characterization is required to identify the individual effect of different noise and vibration sources. The analysis of gas emissions also provides information of possible failures. But emissions are affected by the operation of exhaust aftertreatment systems, air intake defects and by fuel injection pressure, timing and dosing problems, not only by cylinder compression [4], [5]. Starter system performance can be used as a non-invasive, fast and low-cost alternative for diagnosing engines [4].

The starting system is responsible for overcoming the mechanical losses, the inertia of the moving parts and the compression of the cylinders to drive the engine to a speed where the pressure and temperature conditions are adequate for the combustion process to occur [11]. The starting process in diesel engines is affected by factors that influence the temperature and compression pressure inside the combustion chamber such as engine coolant and ambient temperature [12]–[18], crankshaft speed [13], lubricant properties [18], gas leakage during the compression process [19]–[21], timing, pressure, dosage and fuel type [1], [16]; starting system performance [1], [18] and some engine design characteristics such as compression ratio and piston diameter [19], [21]. On the other hand, engine wear and usage have an effect on the starting process, especially at low temperatures [15]. The connections between the above factors are presented in Figure 1.
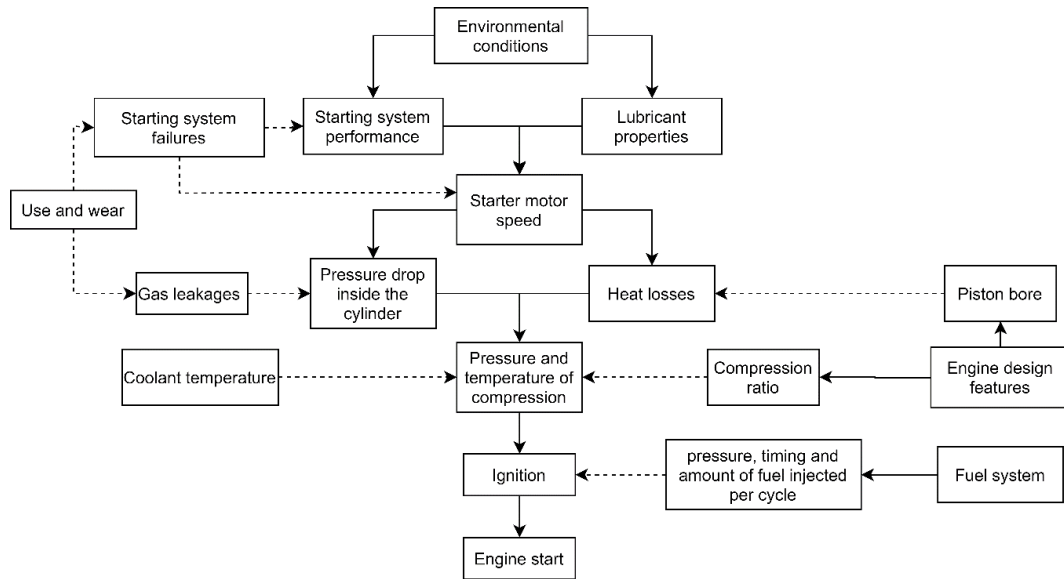
Fig. 1. Factors that affect the starting process.

Many of the studies related to the analysis of the starting system performance of ICE focuses on the diagnosis of the starter motor and/or the battery, based on measurements or modelling of current and voltage [22]–[28]. Related to the analysis of the engine operation during the starting process, Cheng et al. [19] evaluated the effect of blow-by on the indicated mean effective pressure (IMEP) during the cold start process using two four-cylinder diesel engines of 1800 and 1900 cm³, obtaining that due to the low crankshaft speed in the first cycles, the blow-by losses increase because the gases have more time to escape from the chamber and as a consequence the IMEP is reduced. Also, the blow-by was reduced by about 10% at low speed by modifying the first compression ring end clearance. The low-speed blow-by is also investigated theoretically by Rao et al. [21]. The developed model predicts that the blow-by is reduced by about 9% by increasing the speed from 250 min^{-1} to 1000 min^{-1}. Also, the effect of additional combustion chamber volume generated by clearances was investigated, finding decreases in maximum compression pressure and temperature due to increased chamber volume and decreased compression ratio. Henein [20] performs in-cylinder pressure and crankshaft speed measurements with top dead centre detection on two diesel engines, a single-cylinder air-cooled 4T and a six-cylinder water-cooled 2T, obtaining reductions of around 12% in blow-by leakage increasing the crankshaft speed from 250 min^{-1} to 1100 min^{-1}. It was found that due to leakage, the maximum temperature in the combustion chamber is decreased, leading to misfiring. Pszczólkowski [13] correlates the ambient temperature with the minimum conditions of engine speed, injection pressure and air charge at the start of fuel injection of various ICE, finding that as the temperature decreases, the minimum engine speed and compression to start the engine must be higher. However, no relationships are made in those works

with the starting system performance. In other works, variations in the current and voltage of the starting system due to failures or changes in the configuration of the ICE are detected. Moore [4], identifies the effects of a cylinder leakage and a misfire on the starting system performance, obtaining that the current is decreased by about 30% due to leakage, and the stabilization of the crankshaft speed is delayed by about 0.1 s. Due to the misfiring, there is no effect on the current, but a delay in the stabilization of the crankshaft speed of about 0.5 s is observed. Caban et al. [1] investigate the effects of fuel dosing of a 505 cm³ single-cylinder diesel engine on some starting system performance characteristics, the tests are performed at a temperature around 20 ˚C and find that as the fuel dosing increase the voltage drop at the beginning of the starting process increases by 2.3% due to the additional amount of fuel being atomised in the combustion chamber, imposing an additional compressive load and causing that the in-cylinder pressure increase about 1.2% in the first cycle. In these works, the cold start process is analysed in a single engine and invasive variables, such as combustion chamber pressure or blow-by, are measured and adaptations or modifications are required to install the gauges. The measurement of invasive variables can complicate the experiments if several engines are to be used. Bayir [25], presents a graphic patter of voltage versus current that indicates an ICE failure. In this case the engine failure is not specified.

In this work, ten diesel engines of buses of the Megabús transport system in the city of Pereira, Colombia, are diagnosed by analysing and characterizing the signals of battery voltage, starter motor current and crankshaft revolutions during cold and warm start processes. The vehicles tested have different mileages since the last engine repair and differences are found in the starting system

performance of the vehicles with higher mileage attributable to engine wear due to use.

In the following sections, the methodology of the experiment is presented, including the specifications of the engines used, the instrumentation and the particularities of the voltage, current and revolutions signals that carry relevant information of the engine condition. The results are then presented, comparing the performance of the starting system of some of the engines and plotting the magnitudes of the selected characteristics for each vehicle tested. Finally, the relationship of the starting system performance versus vehicle mileage and shutdown time is presented.

2. METHODOLOGY

To experimentally relate the starting characteristics of the engines and their technical-mechanical condition, the electrical variables of the starting system and the instantaneous crankshaft revolutions have been measured. The measurements were carried out on the engines of ten buses of the Megabús transport company. All vehicles are equipped with Isuzu 4HG1 engines, the specifications are presented in Table 1. Information of the mileage travelled by the vehicles after the last engine repair is available, Table 2.

Table 1. Isuzu 4HG1 engine specifications

Motor Isuzu 4HG1	
Type	In-line four-cylinder - 8 valves - OHC - Turbocharged - Water-cooled engine
Displacement [cm³]	4570
Bore x Stroke [mm]	115 x 110
Compression ratio	19:1
Max power [kW]	89 at 3200 min⁻¹
Max torque [Nm]	304 at 1600 min⁻¹
Fuel type	Diesel
Fuel system	Direct injection with mechanically controlled in-line pump
Fuel injection pressure	18.1 MPa
Fuel injection timing	9° before top dead centre
Lubricant	15W-40
Batteries (CCA - CR)	2 batteries - Willard 27AI-100 12 V parallel-connected (670 A – 140 min)
Starter system	Electric 12 V de 3.0 kW (Denso 18500n)

Table 2. Vehicles tested and mileage travelled post-repair

Vehicle	Mileage [km]	Vehicle	Mileage [km]
Vh 1	89880	Vh 6	2386
Vh 2	192902	Vh 7	98323
Vh 3	323355	Vh 8	335950
Vh 4	4788	Vh 9	343851
Vh 5	404337	Vh 10	234274

The vehicles are randomly selected, but prior to the tests, the starting system is checked for correct operation and visual inspection of the engine joints are made to verify the absence of lubricant and fuel leaks. The fuel pressure and injection timing are set according to the manufacturer's specifications. The measurements are carried out during cold engine start processes, at an average ambient temperature of 23 ˚C and then during warm start, at an engine temperature of about 70 ˚C, each process is repeated twice. The engine warm-up time is 25 minutes.

2.1. Instrumentation and data acquisition system

This section presents the instrumentation and data acquisition system used. The variables measured are non-invasive, i.e., no intervention on the tested engines is required to collect the signals, which avoids adapting or modifying parts of the ICE. In each starting process, the battery voltage is measured by means of cables connected to the positive and negative terminals, the current demanded by means of the voltage drop in a 0.75 mΩ shunt connected in series to the common negative terminal of the batteries, and the crankshaft speed and engine block temperature data by means of a capacitive sensor and a thermistor inherent to each engine. The signals are acquired at a frequency of 51.2 kS/s with a NI cDAQ 9174 system equipped with NI9222 and NI9232 cards, both with 16-bit resolution, the specifications of the instruments and the data acquisition system are presented in Table 3. The instrumentation and sensor connection scheme is presented in Figure 2.
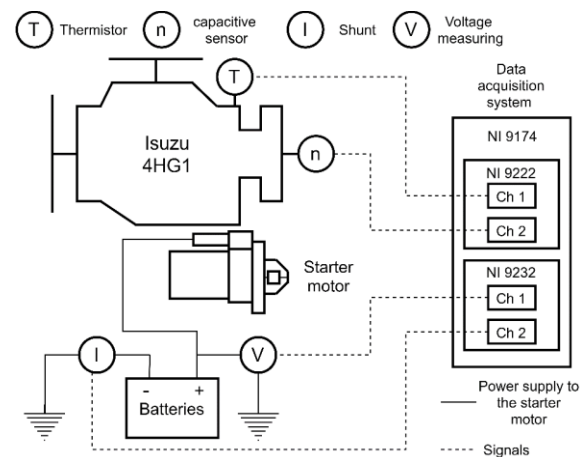

Fig. 2. Equipment connection scheme

2.2. Particularities of the starting process

This section describes the development of the starting process, identifying the particularities of voltage, current and rotational speed signals that carry relevant information to diagnose the ICE.

An example of battery voltage, electrical current and crankshaft rotation speed graphs obtained during a starting process is shown in Figure 3.

Table 3. Instrumentation and data acquisition system specifications

Measuring instruments		
Sensor	Range	Sensitivity
Thermistor	< 400 ºC	Non-linear response
Capacitive sensor	0-8 V	20.5°/pulse
Shunt		0.75 mV/A

Data acquisition system				
Device	Sampling rate	Resolution	Acquired signals	Range
NI 9188 DAQ	51.2 kS/s			
NI 9222	51.2 kS/s	16 bits	Temperature, rotational speed	±10 V
NI 9232	51.1 kS/s	16 bits	Voltage, current	±25 V

In this work, the starting process is divided into four stages. In the first stage the starter motor is energised, causing the starter solenoid to push the gear to engage with the flywheel, initially the maximum battery current (I_{max}) is requested by starter motor to provide the maximum torque and overcome the static friction and engine inertia, also causing the maximum drop in battery voltage (V_{dif}). As the engine accelerates the electric current decreases rapidly until it has a slight increase (I_1) due to the first compression process, accompanied by a voltage drop (V_1). In the second stage, after overcoming the first compression peak, by actuation of the starting system and the impulse provided by the expansion process, the rotational speed increases with an approximately constant acceleration (α_1). In the third stage, the crankshaft acceleration decreases due to the second compression event, which causes an increase in current (I_2) and a voltage drop (V_2).
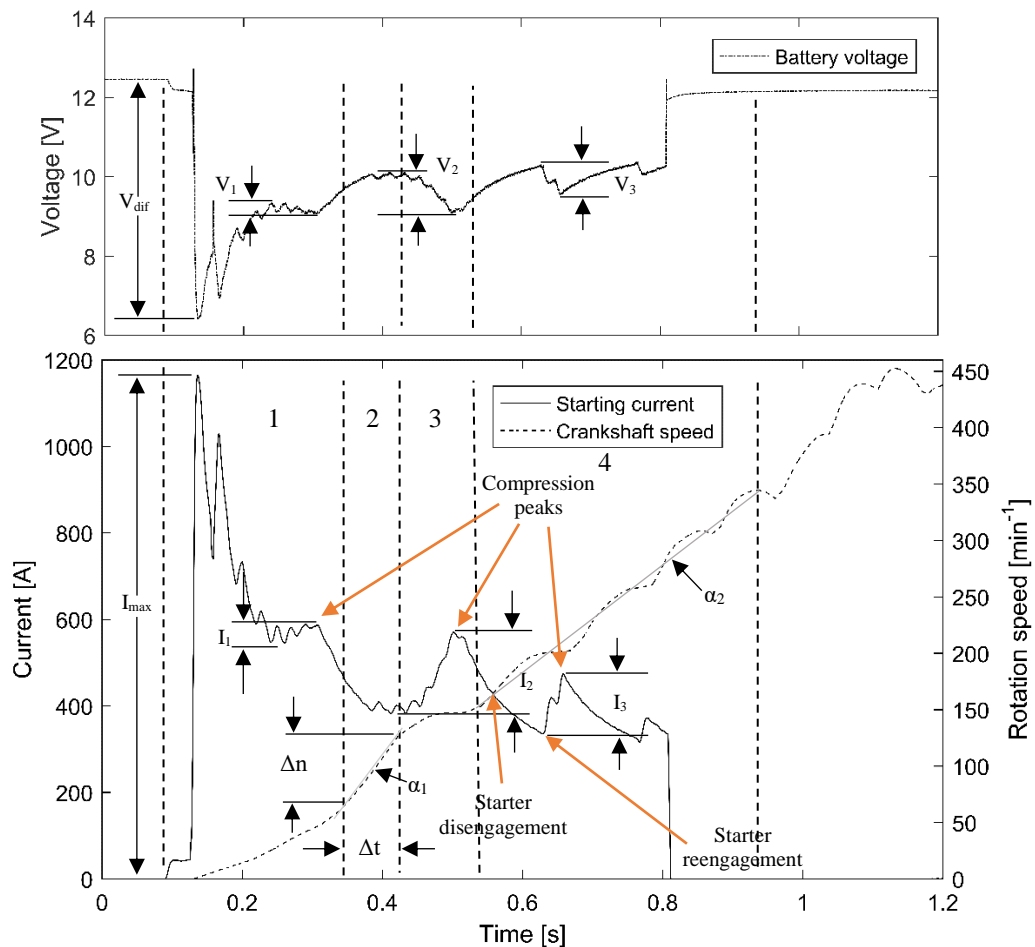

Fig. 3. Graphs of battery voltage, electric current and crankshaft rotation speed versus time during a starting process
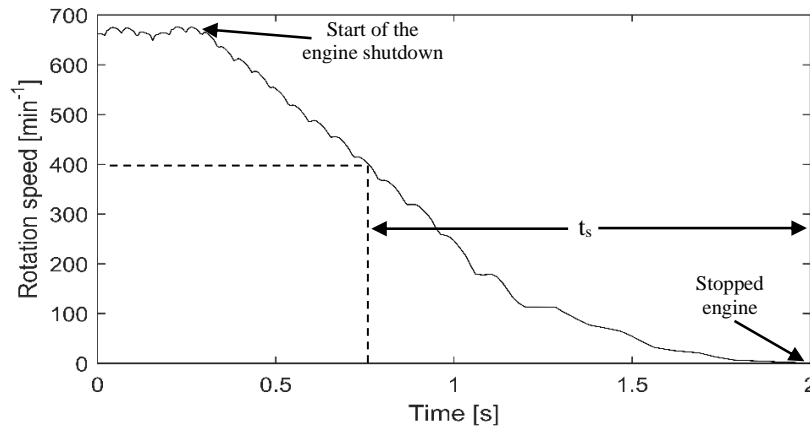
Fig. 4. Engine speed curve during engine shutdown

Subsequently, because of the combustion energy, the rotational speed is increased again with a mean angular acceleration (α_2) and the starter motor is disengaged. If there are problems igniting the fuel (misfire) or the combustion energy is insufficient to start the ICE, the starter motor is re-engaged to help overcome the resistance of the third compression process, requiring additional current (I_3) and causing a voltage drop (V_3). At the end of the fourth stage of the starting process the combustion energy continues to drive the ICM to the stabilization speed. The angular accelerations are calculated using the equation (1).

$$\alpha = \frac{2\pi}{60} \times \frac{\Delta n}{\Delta t} \qquad (1)$$

2.3. Engine shutdown process

Because vehicle mileage is a reference of use and an indicator of engine wear, but that wear also depends on the quality of maintenance, the way in which the vehicle is driven, among other factors, it is aimed to compare the performance of the starting system with another operating characteristic. To infer the condition of the engine, the shutdown process can also be used. When the engine is operating at idle speed and the fuel flow is interrupted, the engine starts to decelerate due to cylinder compression and mechanical losses, Figure 4. As an engine wears out, it takes longer to shut down, because compression restrictions are reduced by leakages. The time it takes for each engine to shut down from an engine speed of 400 min^{-1} is taken as a reference.

3. RESULTS AND ANALYSIS

This section presents the experimental results of the characteristics shown in the current, voltage and crankshaft speed graphs. Initially, only the starting curves of the first five vehicles tested are graphed to enhance the visualization and facilitate analyses of the particularities of the signals. The engine shutdown time as a function of mileage is presented. Subsequently, the characteristics measured in all the engines during the cold and warm starting processes are plotted.

3.1. Starting system performance curves

The current, voltage and crankshaft speed curves for the first five vehicles tested are presented in Figure 5. The battery voltage values before the starting process are between 12.5–12.9 V with cold engine and between 13.2–13.7 V when warm engine, indicating that during the warm-up period the batteries received some electrical charge. For these five vehicles, the voltage drop of the batteries varies between 5.9–6.4 V in the cold start process and between 6.2-6.8 V when the engine is warm. The peak current varies between 1079–1172 A when the engine is cold and between 1146–1197 A when the engine is warm, indicating that in the warm starting process the batteries have the capacity to deliver higher current due to the charge received during the warm-up period. The first engine compression peak current of the first five vehicles is around 550 A in the cold start period and around 600 A in the warm start process, because during the warm-up period the engine parts expand and the oil fill the clearances between the piston, rings, and cylinder, therefore, the blow-by leakage is reduced, improving the compression of the engine, and demanding more torque from the starter motor. The crankshaft speed at the end of the second stage of the cold start process is close to 140 min^{-1} while in the warm start process it is close to 160 min^{-1} due to the additional impulse of the first expansion process, resulting from the leakage reduction. The current growth I1 and voltage drop V_1 vary between 38.1–76.7 A and 0.3–0.45 V in the cold start process and between 30.9–57.4 A and 0.13–0.32 V in the warm start process.

Analysing the peak current I_2 variations between 172–218 A can be observed when the engine is cold, obtaining the maximum value with the engine of vehicle 4. which has travelled 4788 km since the last repair and the minimum value with the engine of vehicle 3 which has travelled more than 300000 km, which in accordance with the results of Moore [4], indicates the presence of greater leakage in the engine of vehicle 3. When the engines are warmed

up I_2 varies between 155–177 A. The additional boost from the first expansion process and the reduction of friction losses due to the decrease in oil viscosity explains why the peak current I_2 is lower when the engine is warm, i.e., less torque is required from the starter motor in this compression process. On the other hand, the voltage drop V_2 varies between 0.99–1.22 V at cold start and between 0.86–1.02 V at warm start.

Regarding the I_3 current, it varies between 36.5–146.6 A when the engines are cold. The engines of vehicles 3 and 5 require the most assistance from the starter motor in the third compression process and are also the vehicles with the most kilometres driven. Due to leakage, these engines have the highest IMEP losses and possible misfiring. In the warm start process, I_3 varies between 0–87.5 A, in this case engines of vehicles 1. 2 and 4 show no current growth in the third compression stroke, i.e., the combustion occurring in the second compression stroke is sufficient to continue driving the ICE, while engines of vehicles

3 and 5 still require assistance from the starter system. As an additional characteristic of the starting system performance of these five engines, vehicles 3 and 5. with 323355 km and 404337 km travelled respectively, show four compression peaks during cold start and three during warm start, while the other engines show three peaks during cold start and two during warm start. The voltage drop V_3 varies between 0.21–0.78 V and 0–0.5 V for the cold and warm start processes respectively.

About the growth of crankshaft rotation speed in the fourth stage of the starting process, in cold and warm conditions, the crankshaft speed of vehicles with lower mileage grows and stabilise more quickly, because they have less IMEP loss due to blow-by leakage and less difficulty in igniting the injected fuel. It can also be observed, especially in the cold start process, that the engines with higher mileage start to stabilise the speed after 0.9 s and that the stabilised speeds are lower than 450 min^{-1} while the other engines stabilise the speed at around 0.7 s and at speeds around 500 min^{-1}.
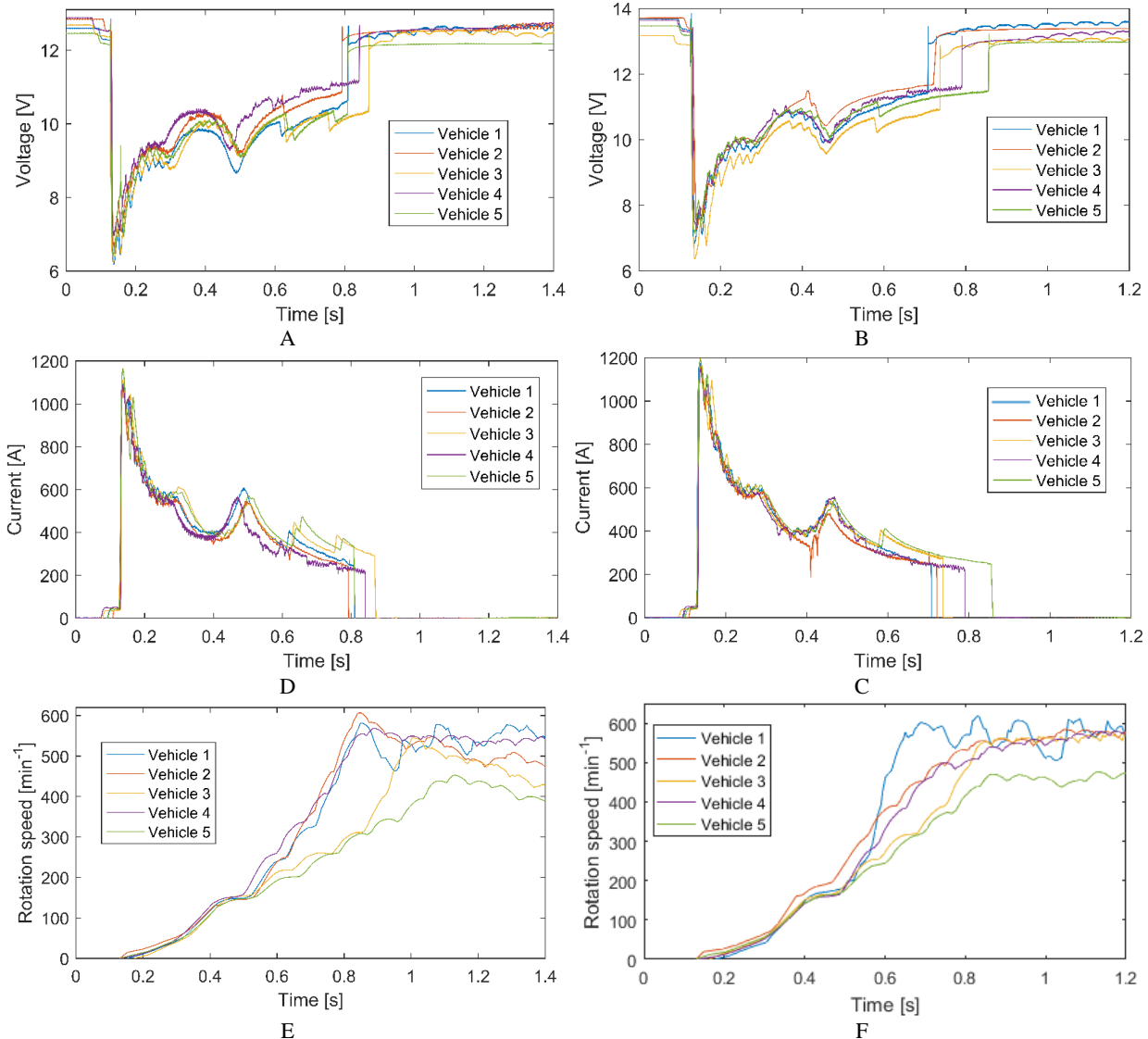

Fig. 5. Curves of the starting process. A. cold start voltage, B. warm start voltage; C. cold start current, D. warm start current, E. rotation speed at cold start, F. rotation speed at warm start

This, according to Droździel and Krzywonos [15], is related to the wear of the engines caused by

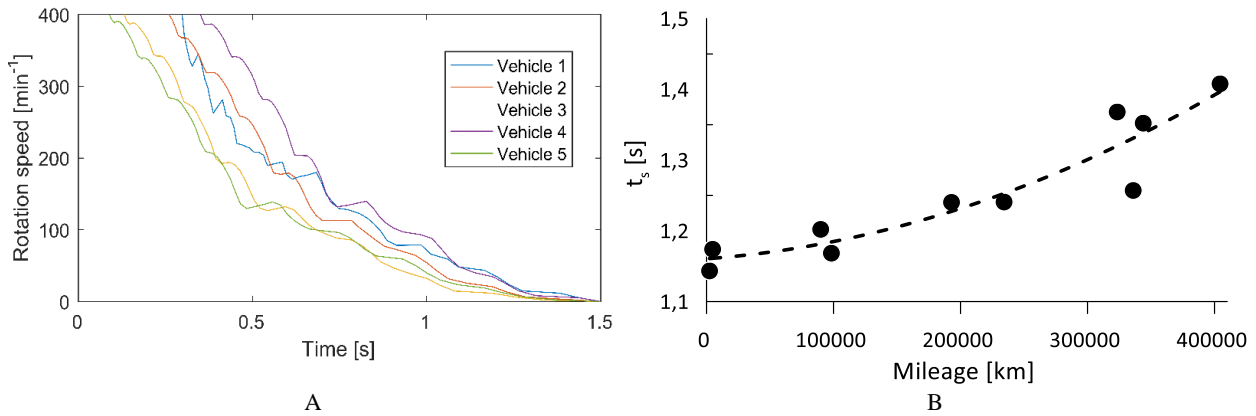use or travel, extending the duration of the starting process.

Fig. 6. Shutdown process. A. speed versus time of the first five vehicles, B. shutdown time versus mileage
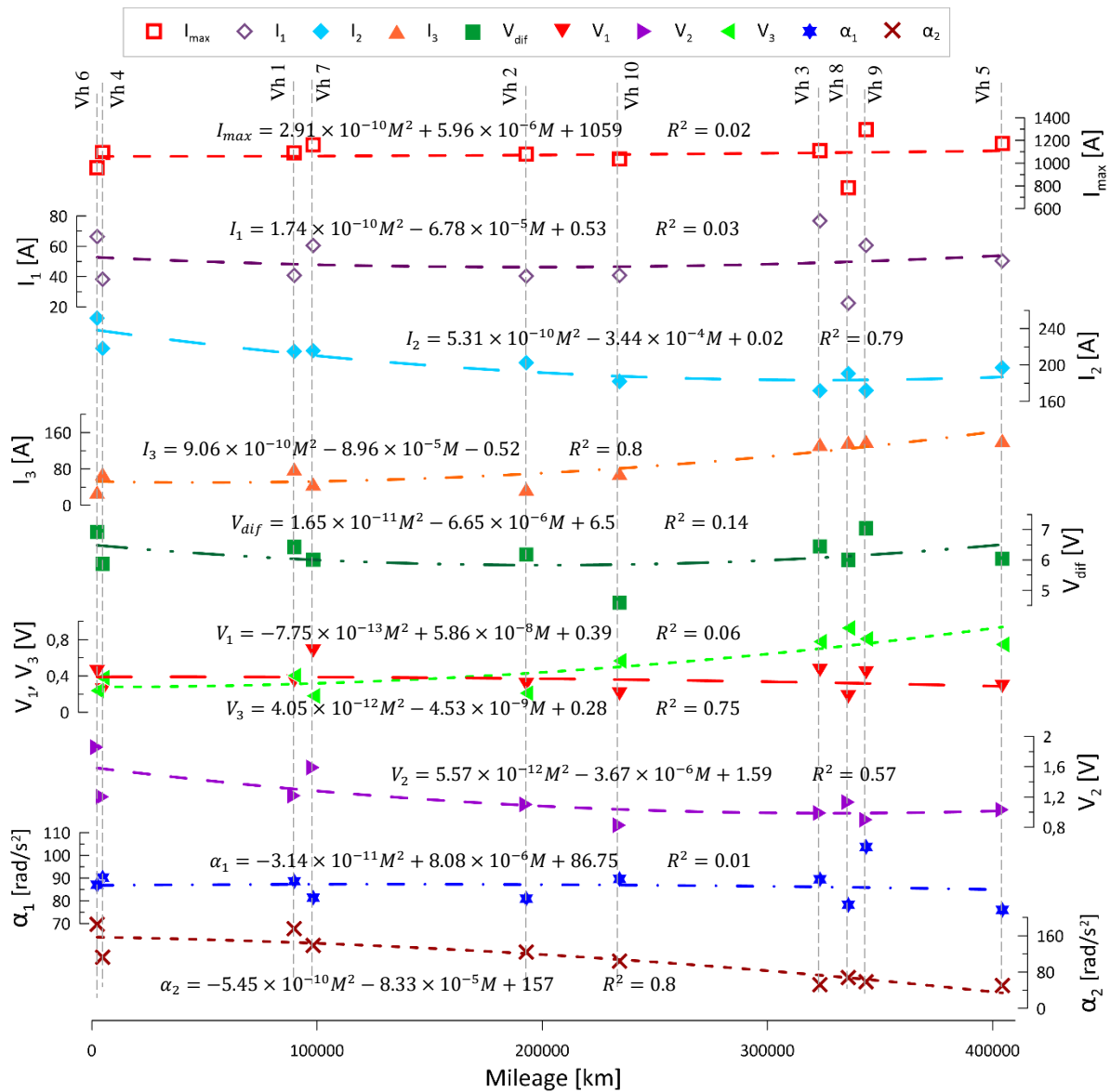

Fig. 7. Cold engine starting system performance characteristics

3.2. Engine shutdown time

This section presents the results related to the shutdown process, which is an additional indicator of engine wear. Figure 6 shows the curves of crankshaft rotation speed versus time during the engine shutdown process only for the first five buses tested to enhance the visualization. It can be seen that for vehicles 3 and 5. it takes about 1.4 s to stop from a speed of 400 min$^{-1.}$ the other engines stop within 1.2 s. A graph of the shutdown time against the mileage of all the tested vehicles is also presented, where an increasing tendency of the shutdown time is observed as the engines are used, this is due to the fact that wear causes compression losses, so the engines can rotate with less restriction when it is shutting down. The equation (2) corresponds to the curve fitted in the Figure 6B, where t_s is the time to stop and M is the vehicle mileage.

$$t_s = 1.16 + 1.32 \times 10^{-7}M + 1.18 \times 10^{-12}M^2 \quad (2)$$
$$R^2 = 0.87$$

3.3. Characteristics of the starting process

In this section, graphs of the starting process characteristics measured for each engine are presented. Figure 7 shows the superposition of the cold start process characteristics versus the vehicle mileage, while in Figure 8 are presented the warm start process characteristics. A trend curve, as a function of mileage, is fitted to each characteristic. The equations and the coefficients of determination (R^2) are plotted in the Figure 7 and Figure 8 near the corresponding curve. The highest R^2 are obtained with the curves of characteristics I_2, I_3, V_3 and α_2, between 0.75 and 0.8 for cold start and between 0.4 and 0.85 for warm start.
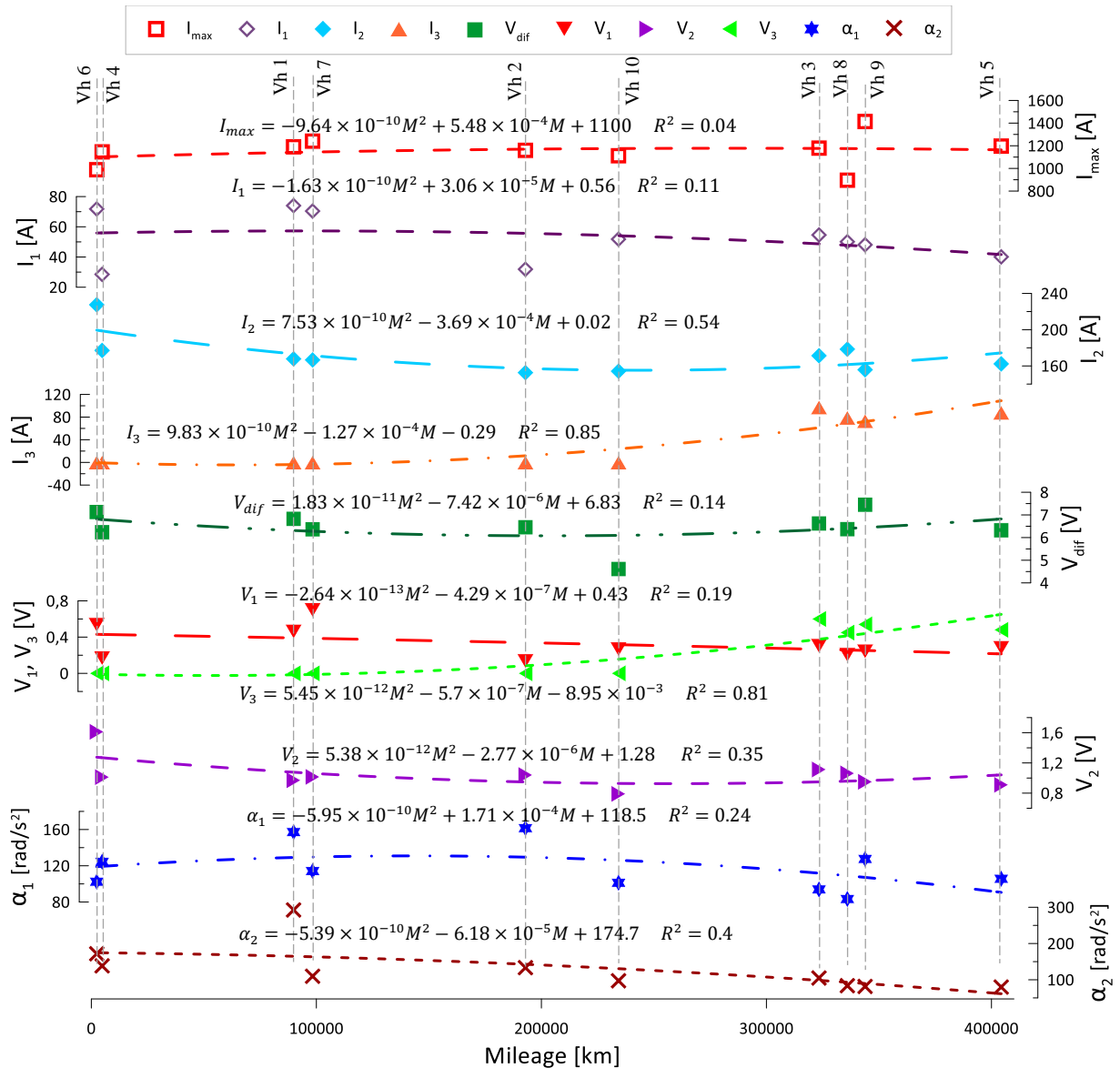

Fig. 8. Warm engine starting system performance characteristics

Observing the current variations, engines of vehicles with less than 100000 km travelled require more than 215 A to overcome the second compression process (I_2). The compression of engines with longer travel demands less current. Due to combustion problems, engines with more than 300000 km require more assistance from the starter motor in the third compression process, causing an increase in current (I_3) of more than 134 A and due to difficulties igniting the fuel the mean angular acceleration (α_2) is also slower, less than 68 rad/s². Furthermore, it is observed that the voltage drop of the batteries in the third compression process is higher, reaching up to 0.93 V in the cold start process and 0.54 V in the warm start process. Of the other characteristics, no trend related to vehicle mileage or shutdown time is observed.

Figure 8 shows the characteristics of the warm start processes. In this case, the current of the second compression process (I_2) is only remarkable for the engine of vehicle 6 with 227 A, this is the vehicle

with the lowest mileage since the last repair, while in the remaining vehicles the current varies between 155–178 A. In the third compression peak, only in vehicles with mileage over 300000 km, engines require assistance from the starting system (I_3), i.e., that there are combustion problems during the start process even with warmed-up engine, causing an increase in current of between 73–98 A. Therefore, the growth of the crankshaft rotational speed of these vehicles is slower, the mean angular acceleration (α_2) is less than 109 rad/s².

Figure 9 presents the current characteristics of the second compression process (I_2), current of the third compression process (I_3), voltage drop of the third compression process (V_3) and angular acceleration in the fourth stage of the starting process (α_2) graphed against the shutdown time of the ICE and the mileage of the vehicles. In the graphs, the blue surfaces are fitted to the experimental cold start data and green surfaces to warm start.
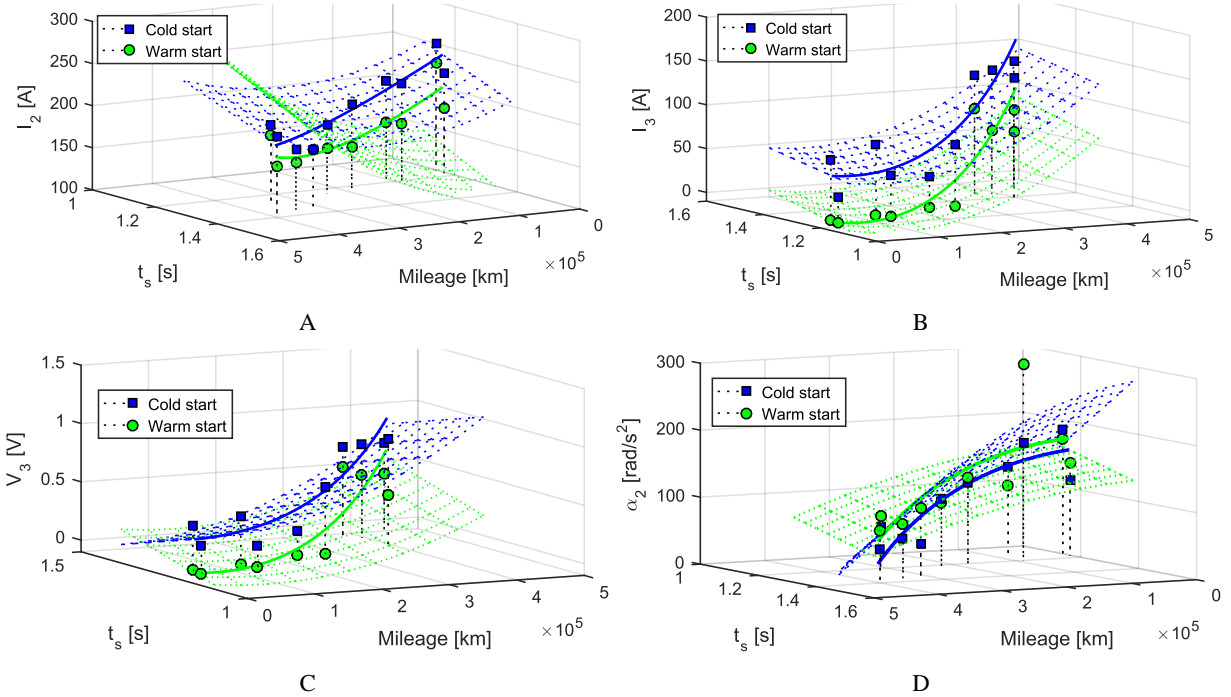

Fig. 9. Variation against shutdown time and vehicle mileage of A. current I_2. B. current I_3.
C. voltage drop V_3 and D. angular acceleration α_2

Table 4. Equations of surfaces

Characteristic	Condition	Equation	
I_2	Cold start	$I_2 = 414.2 - 3.2 \times 10^{-4}M - 150.9\,t_s + 7 \times 10^{-10}M^2$	$R^2 = 0.83$
	Warm start	$I_2 = 417.8 - 3.4 \times 10^{-4}M - 187.4\,t_s + 9.6 \times 10^{-10}M^2$	$R^2 = 0.62$
I_3	Cold start	$I_3 = -27.6 - 9.9 \times 10^{-5}M + 68.9\,t_s + 8.8 \times 10^{-10}M^2$	$R^2 = 0.85$
	Warm start	$I_3 = -103.8 - 1.4 \times 10^{-4}M + 89.2\,t_s + 8.3 \times 10^{-10}M^2$	$R^2 = 0.8$
V_3	Cold start	$V_3 = 1.44 + 1.3 \times 10^{-7}M - t_s + 5.2 \times 10^{-12}M^2$	$R^2 = 0.76$
	Warm start	$V_3 = -1.04 - 6.9 \times 10^{-7}M + 0.89\,t_s + 4.4 \times 10^{-12}M^2$	$R^2 = 0.82$
α_2	Cold start	$\alpha_2 = 301 - 6.7 \times 10^{-5}M - 124.1\,t_s + 4.1 \times 10^{-10}M^2$	$R^2 = 0.81$
	Warm start	$\alpha_2 = -367.8 - 1.2 \times 10^{-5}M + 467.5\,t_s + 1.1 \times 10^{-9}M^2$	$R^2 = 0.46$

The equations of the surfaces are presented in Table 4. In Figure 9. continuous lines are plotted too. That lines are obtained replacing the equation (2) in the equation of each surface.

4. CONCLUSIONS

The engines of ten buses of the Megabús transport company were diagnosed by means of the starting system performance. Signal characteristics of battery voltage, current and crankshaft rotation speed related to the compression of the cylinders and the state of each engine were identified. The characteristics were related to vehicle mileage and engine shutdown time. The analyses of starting process curves were made only for the first five engines tested, but the characteristics were identified for all the engines.

The engine shutdown time was related to the kilometres travelled after the last engine repair. Due to increased leakage caused by wear, engines with higher usage take more time to stop from an engine speed of 400 min^{-1} due to less restriction of cylinder compression.

It was found that the growth of the current demanded by the starter motor in the second compression peak during the cold start process is higher in engines of vehicles with lower mileage, being higher than 215 A in engines of vehicles with less than 100000 km. The current growth at the third compression peak is higher in engines with higher mileage due to the higher starter motor assistance required due to fuel ignition problems in the second compression process and the IMEP loss. During the warm start process only engines with more than 300000 km require starter assistance in the third compression ratio. In addition, due to combustion problems, the crankshaft speed growth in the fourth stage of the starting process is slower, which prolongs the starting process and delays the stabilisation of the crankshaft rotational speed.

ACKNOWLEDGEMENTS

Author contributions: *research concept and design, J.D.R, C.A.R., H.F.Q.; Collection and/or assembly of data, J.D.R., J.C.M.; Data analysis and interpretation, J.D.R., C.A.R.; Writing the article, J.D.R.; Critical revision of the article, C.A.R., J.C.M., H.F.Q.; Final approval of the article, C,A.R.*

Declaration of competing interest: *The authors declare that they have no known competing financial interests or personal relationships that could have appeared to influence the work reported in this paper.*

REFERENCES

1. Caban J, Droździel P, Ignaciuk P, Kordos P. Analysis of the effect of the fuel dose on selected parameters of the diesel engine start-up process. Transportation Research Procedia. 2019;40:647–654. https://doi.org/10.1016/j.trpro.2019.07.092
2. Delvecchio S, Bonfiglio P, Pompoli F. Vibro-acoustic condition monitoring of Internal Combustion Engines: A critical review of existing techniques. Mechanical Systems and Signal Processing. 2018;99:661–683. https://doi.org/10.1016/j.ymssp.2017.06.033
3. Hudec J, Šarkan B, Czodörová R. Examination of the results of the vehicles technical inspections in relation to the average age of vehicles in selected EU states. Transportation Research Procedia. 2021;55:2–9. https://doi.org/10.1016/j.trpro.2021.07.063
4. Moore DJ. Condition monitoring of diesel engines. University of Manchester; 2013.
5. Jones NB, Li YH. A review of condition monitoring and fault diagnosis for diesel engines. Tribotest Journal. 2000;6(3):267–291. https://doi.org/10.1002/tt.3020060305
6. Basurko O, Uriondo Z. Condition-based maintenance for medium speed diesel engines used in vessels in operation. Applied Thermal Engineering, 2015; 80: 404–412. https://doi.org/10.1016/j.applthermaleng.2015.01.075
7. Palomo Guerrero D, Jiménez-Espadafor FJ. Torsional system dynamics of low speed diesel engines based on instantaneous torque: Application to engine diagnosis. Mechanical Systems and Signal Processing. 2019;116:858–878. https://doi.org/10.1016/j.ymssp.2018.06.051
8. Grajales JA, Quintero HF, López JF, Romero CA, Henao E, Cardona O. Engine diagnosis based on vibration analysis using different fuel blends. Diagnostyka. 2017;18(4):27–36.
9. Barelli L, Barluzzi E, Bidini G, Bonucci F. Cylinders diagnosis system of a 1MW internal combustion engine through vibrational signal processing using DWT technique. Applied Energy. 2012;92:44–50. http://dx.doi.org/10.1016/j.apenergy.2011.09.040
10. Kim H-W, Lee S-K. Diagnosis of engine misfiring based on the adaptive line enhancer. IFAC Proceedings Volumes. IFAC; 2008;41:85–89. https://doi.org/10.3182/20080706-5-KR-1001.00014
11. Robert Bosch GmbH. Automotive electrics and automotive electronics. Bosch Professional Automotive Information. 2007.
12. Xiao GF, Qiao XQ, Huang Z, Chen ZP. Improvement of startability of direct-injection diesel engines by oxygen-enriched intake air. Proceedings of the Institution of Mechanical Engineers, Part D: Journal of

Automobile Engineering. 2007;221(11):1453–1465. https://doi.org/10.1243/09544070JAUTO541

13. Pszczółkowski J. Multidimensional engine starting characteristics. Journal of KONES Powertrain and Transport. 2010;17(3):385–92.

14. Henein NA, Zahdeh AR, Yassine MK, Bryzik W. Diesel engine cold starting: Combustion instability. SAE Technical Papers. 1992:920005. https://doi.org/10.4271/920005

15. Droździel P, Krzywonos L. Ocena niezawodnosci pierwszego dziennego rozruchu silnika o zaplonie samoczynnym w warunkach uzytkowania pojazdu. Eksploatacja i Niezawodnosc. 2009;41(1):4–10.

16. Chaichan MT. Effect of injection timing and coolant temperatures of DI diesel engine on cold and hot engine startability and emissions. IOSR Journal of Mechanical and Civil Engineering (IOSRJMCE). 2016;13(3-6):62–70. https://doi.org/10.9790/1684-1303066270

17. Celik A, Yilmaz M, Yildiz OF. Improvement of diesel engine startability under low temperatures by vortex tubes. Energy Reports. 2020;6:17–27. https://doi.org/10.1016/j.egyr.2019.11.027

18. Gupta RB. Cold starting of IC engines. Defence Science Journal. 1988;38(1):77–85. https://doi.org/10.14429/dsj.38.4827

19. Cheng KY, Shayler PJ, Murphy M. The influence of blow-by on indicated work output from a diesel engine under cold start conditions. Proceedings of the Institution of Mechanical Engineers, Part D: Journal of Automobile Engineering. 2004;218(3):333–340. https://doi.org/10.1243/095440704322955858

20. Henein NA. Starting of diesel engines: Uncontrolled fuel injection problems. SAE Technical Papers. 1986:(860253). https://doi.org/10.4271/860253

21. Rao VK, Gardiner DP, Bardon MF. Effects of gas leakage and crevices on cold starting of engines. SAE Technical Paper. 1994:940078. https://doi.org/10.4271/940078

22. Puzakov AV, Dryuchin DA, Voinash SA, Ariko SY, Kamenchukov AV, Ukraimsky IS. Diagnostics of automobile starters by the parameter of current consumption. Journal of Physics: Conference Series. 2020;1679(4). https://doi.org/10.1088/1742-6596/1679/4/042043

23. Averbukh M, Rivin B, Vinogradov J. On-board battery condition diagnostics based on mathematical modeling of an engine starting system. SAE Technical Papers. 2007;2007(724). https://doi.org/10.4271/2007-01-1476

24. Bay ÖF, Bayir R. A fault diagnosis of engine starting system via starter motors using fuzzy logic algorithm. Gazi University Journal of Science. 2011;24(3):437–449.

25. Bayir R. Condition monitoring and fault diagnosis of serial wound starter motor learning vector quantization network. Journal of Applied Science. 2008;8:3148–56.

26. Bayir R, Bay ÖF. Serial wound starter motor faults diagnosis using artificial neural network. Proceedings of the IEEE International Conference on Mechatronics 2004. ICM'04. 2004;2:194–199. https://doi.org/10.1109/ICMECH.2004.1364436

27. Mani MV, Chandramohan G, Rudramoorthy R, Senthil KM, Ashok KL. Experimental analysis of faults of automobile starting. Journal of Advances in Vehicle Engineering. 2016;2(2):124–132.

28. Patil AB, Ranade NS. Computer simulation of an I. C. engine during cranking by a starter motor. SAE Technical Paper Series. 1993;412:930626. https://doi.org/10.4271/930626
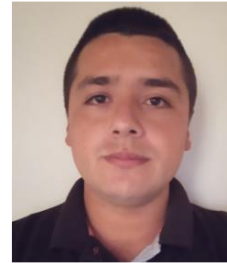
Juan D. RAMÍREZ received Mechanical Engineer degree from Pereira Technological University, Pereira, Colombia, in 2017. Now he works at Pereira Technological University and he is Mechanical Engineering M.Sc. student at Pereira Technological University. His current research interests include Internal combustion machine, and machine design.

Carlos A. ROMERO received Ph.D. degree in Mechanical Engineering from Valencia Polytechnic University, Valencia, Spain, in 2009. Now he works at Pereira Technological University. His current research interests include internal combustion machine, and machine design.

Juan C. MEJÍA received M.Sc. degree in Electrical Engineering from Pereira Technological University, in 2019. Now, he is Professor at Pereira Technological University. His current research interests include instrumentation, digital systems programming, signal processing and machine learning algorithms.

Héctor F. QUINTERO received Ph.D. degree in Mechanical Engineering from Cataluña Polytechnic University, Barcelona, Spain, in 2006. Now he works at Pereira Technological University. His current research interests include analysis and synthesis of mechanisms, mechanical vibrations and fault diagnosis.